Identification of marine and continental aerosol sources in Paris using high resolution aerosol mass spectrometry

Monica Crippa, Imad El Haddad, Jay G. Slowik, Peter F. Decarlo, Claudia Mohr, Maarten F. Heringa, Roberto Chirico, Nicolas Marchand, Jean Sciare, Urs Baltensperger, et al.

▶ **To cite this version:**

Monica Crippa, Imad El Haddad, Jay G. Slowik, Peter F. Decarlo, Claudia Mohr, et al.. Identification of marine and continental aerosol sources in Paris using high resolution aerosol mass spectrometry. Journal of Geophysical Research: Atmospheres, 2013, 118 (4), pp.1950 - 1963. 10.1002/jgrd.50151 . hal-01663090

HAL Id: hal-01663090
https://hal.science/hal-01663090v1

Submitted on 17 Sep 2020

HAL is a multi-disciplinary open access archive for the deposit and dissemination of scientific research documents, whether they are published or not. The documents may come from teaching and research institutions in France or abroad, or from public or private research centers.

L'archive ouverte pluridisciplinaire **HAL**, est destinée au dépôt et à la diffusion de documents scientifiques de niveau recherche, publiés ou non, émanant des établissements d'enseignement et de recherche français ou étrangers, des laboratoires publics ou privés.

JOURNAL OF GEOPHYSICAL RESEARCH: ATMOSPHERES, VOL. 118, 1950–1963, doi:10.1002/jgrd.50151, 2013

Identification of marine and continental aerosol sources in Paris using high resolution aerosol mass spectrometry

Monica Crippa,[1] Imad El Haddad,[1] Jay G. Slowik,[1] Peter F. DeCarlo,[1,4] Claudia Mohr,[1,5] Maarten F. Heringa,[1,6] Roberto Chirico,[1,7] Nicolas Marchand,[2] Jean Sciare,[3] Urs Baltensperger,[1] and André S. H. Prévôt[1]

Received 20 August 2012; revised 5 November 2012; accepted 25 November 2012; published 19 February 2013.

[1] Major summertime aerosol emission sources in Paris were assessed using a high resolution time-of-flight aerosol mass spectrometer (HR-ToF-AMS). The application of positive matrix factorization (PMF) to the highly mass and time-resolved AMS measurements allowed the identification of primary and secondary sources of organic (OA) and sulfate aerosols. Primary anthropogenic emissions contributed on average ~27% (14.7% cooking, 12% traffic) to the total organic mass, while the major contribution to the organic fraction was associated with secondary formation products. Low-volatility oxygenated OA (LV-OOA, 25.2%) and semi-volatile oxygenated OA (SV-OOA, 32.4%) factors were classified as SOA. An additional component with high S : C and O : C ratios was identified and attributed to marine emissions (marine organic aerosol, MOA), owing to its high correlation with methanesulfonic acid ($R^2 = 0.84$) and contributing on average 15.7% to the total OA mass, even in the continental megacity of Paris. Non-sea salt sulfate was apportioned by including both organic and sulfate ions in the PMF data matrix. This allowed apportionment of submicron sulfate to continental versus marine sources. A detailed source apportionment of PM_1 combining AMS, aethalometer, and filter data is presented.

Citation: Crippa, M., et al. (2013), Identification of marine and continental aerosol sources in Paris using high resolution aerosol mass spectrometry, *J. Geophys. Res. Atmos.*, *118*, 1950–1963, doi:10.1002/jgrd.50151.

1. Introduction

[2] Air quality is often a major issue in urban areas, affecting human health, ecosystems, and climate [*Intergovernmental Panel on Climate Change* (*IPCC*), 2007; *Laden et al*., 2000]. Particulate matter (PM) is currently of special interest. PM is a complex mixture including organic matter (organic aerosol, OA), elemental carbon (EC, also termed BC for black carbon), and inorganic species (e.g., ammonium sulfate and nitrate, metals, dust) suspended in the air. Aerosol particles can be emitted directly from primary sources or formed in the atmosphere via the oxidation of gas-phase precursors and subsequent partitioning of the resulting low-volatility products into the particle phase [*Kroll and Seinfeld*, 2008]. The latter fraction is termed secondary aerosols. Primary particles and secondary aerosol precursors can arise from both anthropogenic (e.g., traffic, domestic heating, and industrial activities) and biogenic/natural (e.g., wild fires, volcano, and forests) emissions. An accurate knowledge of the predominant emission sources affecting urban aerosol is needed to design effective mitigation strategies for adverse effects of PM on health, visibility, and climate.

[3] The Aerodyne aerosol mass spectrometer (AMS) [*Canagaratna et al*., 2007] has significantly improved the characterization and source apportionment potential of submicron PM (PM_1). The highly time-resolved mass spectra provided by the AMS enable quantification of the non-refractory inorganic (e.g., NH_4^+, NO_3^-, SO_4^{2-}, and Cl^-) and organic sub-micrometer PM. The application of positive matrix factorization (PMF) to OA mass spectra demonstrates the possibility to describe the spectra in terms of a set of factors corresponding to specific sources or processes

All supporting information may be found in the online version of this article.

[1]Laboratory of Atmospheric Chemistry, Paul Scherrer Institute, Villigen, Switzerland.
[2]Aix-Marseille Université, CNRS, Marseille, France.
[3]Laboratoire des Sciences du Climat et de l'Environnement (LSCE/IPSL), Laboratoire CEA-CNRS-UVSQ, Gif-sur-Yvette, France.
[4]Department of Civil, Architectural, and Environmental Engineering and Department of Chemistry, Drexel University, Philadelphia, Pennsylvania, USA.
[5]Department of Atmospheric Sciences, University of Washington, Seattle, Washington, USA.
[6]WIL Research, 's-Hertogenbosch, The Netherlands.
[7]Italian National Agency for New Technologies, Energy and Sustainable Economic Development (ENEA), UTAPRAD-DIM, Frascati, Italy.

Corresponding author: A. S. H. Prévôt, Laboratory of Atmospheric Chemistry, Paul Scherrer Institute, PSI Villigen, 5232, Switzerland. (andre.prevot@psi.ch)

©2013. American Geophysical Union. All Rights Reserved.
2169-897X/13/10.1002/jgrd.50151.

[*Lanz et al*., 2007; *Lanz et al*., 2010; *Mohr et al*., 2012; *Ulbrich et al*., 2009; *Zhang et al*., 2011]. These factors often include primary OA (POA) from traffic (HOA), biomass burning (BBOA) and cooking (COA), and an oxygenated fraction (OOA) related to secondary OA (SOA). SOA typically is the dominant fraction, even in urban areas [*Zhang et al*., 2007]. OOA is typically classified by degree of oxygenation and volatility as semi-volatile (SV OOA) and low volatility (LV-OOA). Although source-related trends in factor mass spectra have been reported by a number of researchers [e.g., *Heringa et al*., 2012], quantification of SOA from specific sources (e.g., discrimination between biogenic and anthropogenic precursors) is not generally obtained except when local geography and/or meteorology cause highly distinct temporal variations [e.g., *Setyan et al*., 2012].

[4] Covering over two thirds of the Earth's surface, oceans constitute one of the most important natural sources of both primary and secondary aerosols and consequently have significant impacts on the Earth's albedo and climate [*Charlson et al*., 1987; *O'Dowd et al*., 2004]. So far, studies of marine aerosol have focused mostly on the production of aerosol sea salt (mainly sodium chloride) associated with bubble bursting [*Fitzgerald*, 1991] and non-sea-salt sulfate (nss-SO_4^{2-}). Compared to anthropogenic sources from ships and industries, marine emissions overwhelm the marine sulfur global budget through the production of secondary sulfate. This production occurs via the photo-oxidation of DMS (dimethyl sulfide = $(CH_3)_2S$), a product of phytoplankton decomposition [*Seinfeld and Pandis*, 2006]. DMS oxidation yields simultaneously methanesulfonic acid (MSA = CH_3SO_3H) and SO_2, which ultimately evolves into sulfate (nss-SO_4^{2-}) after further oxidation. The sulfur budget is dominated by two main components, deriving from fossil fuel combustion (70 ± 100 Tg S/yr) and from oceanic biological activity (12 ± 58 Tg S/yr). Volcanoes (3 ± 9 Tg S/yr), land biosphere (0.1 ± 7 Tg S/yr), and biomass burning (1 ± 4 Tg S/yr) fluxes are instead much smaller [*Liss et al*., 1997].

[5] However, field experiments have shown that known aerosol production processes for inorganic species cannot explain the significant concentrations of PM in marine aerosol [*Novakov et al*., 1997; *Putaud et al*., 2000; *Quinn et al*., 2000]. Unlike sea salt, marine OA occurs primarily in the submicron fraction of PM and dominates during the spring and summertime phytoplankton bloom, contributing up to 70% of marine PM_1 [*Rinaldi et al*., 2010]. Additionally, evidence for primary marine OA sources has been found in coastal measurements [*Cavalli et al*., 2004; *O'Dowd et al*., 2004; *Russell et al*., 2010; *Sciare et al*., 2009] and bubble-bursting experiments [*Facchini et al*., 2008b]. Detailed analyses, such as nuclear magnetic resonance (NMR) and Fourier transform infrared (FTIR) analyses of marine POA associate this fraction with lipopolysaccharide aggregates, comprising saturated and unsaturated fatty acids [*Decesari et al*., 2011], polyols, and carbohydrates [*Russell et al*., 2010]. While this fraction was often found to be related with water insoluble organic matter, measurements of aged marine air masses show that OA is predominantly water soluble and highly oxygenated, indicating a strong influence of rapid SOA-forming reactions [*Rinaldi et al*., 2010 and references therein]. Of this SOA, MSA typically accounts for less than 20% (according to measurements performed in Mace Head, Ireland). The remaining fraction comprises a complex mixture of sulfate esters, oxo and hydroxyl carboxylic and dicarboxylic acids resulting from the photo-oxidation of unsaturated fatty acids [*Claeys et al*., 2010; *Decesari et al*., 2011; *Mochida et al*., 2002; *Rinaldi et al*., 2010] and biologically emitted methyl amines [*Facchini et al*., 2008a]. This complex mixture of chemical components identified in marine primary and secondary organic aerosol accounts for less than half of the total mass and shows a high variability depending on the season and sampling location [*Rinaldi et al*., 2010]. Furthermore, the evolution of this fraction during atmospheric transport of marine air masses over the continent and its contribution to the total aerosol loading in urban atmospheres remain poorly constrained.

[6] Here, we present results from high-resolution time-of-flight aerosol mass spectrometer (HR-ToF-AMS) measurements conducted during summertime at an urban background site in Paris (20 km far from the Paris city center and not directly exposed to urban emissions), which was impacted by marine air masses coming from the Atlantic Ocean. Results were obtained within the MEGAPOLI project (Megacities: Emissions, urban, regional and Global Atmospheric POLlution and climate effects, and Integrated tools for assessment and mitigation) (M. Beekmann et al., Will regional emissions control fine particulate matter levels in future megacities? submitted manuscript, 2013). An overview of the measurement campaign, aerosol composition, size distribution, and sources over the Parisian region during summertime depending on air masses origin is detailed in *Freutel et al*. [2013]. The objective of this study is to (i) characterize the primary and secondary aerosol sources by applying PMF analysis to HR-ToF-AMS data, with a main focus on marine emissions and (ii) assess the contribution of continental and marine emissions to OA and sulfate for different air mass origins.

2. Experimental

2.1. Sampling Site and General Conditions

[7] An intensive measurement campaign was performed from 1 to 31 July 2009 at the urban background site SIRTA ("Site Instrumental de Recherche par Télédétection Atmosphérique"; latitude 48.71°N, longitude 2.21°E, 60 m above sea level), located at ~20 km SW of Paris [*Haeffelin et al*., 2005]. The SIRTA site is situated in the flat Parisian plain, surrounded by villages, highways, and major roads connecting the suburban areas with the center of Paris. In addition to the effect of local emission sources (such as traffic, cooking, and during wintertime biomass burning), the aerosol mass concentration and chemical composition were strongly affected by regional pollution, as described elsewhere [*Crippa et al*., 2013; *Freutel et al*., 2013].

[8] Back trajectory analysis performed with FLEXPART allowed classification of the air masses impacting the sampling site into three categories: "continental" (air advected from central Europe), "Atlantic polluted," and "Atlantic clean" periods. These Atlantic periods were distinguished by the air residence time over the continent (if the residence time over continental areas was longer than 1 day before sampling, the measurement period was defined as Atlantic polluted), as described by *Freutel et al*. [2013]. Only the

beginning of the campaign was characterized by continental air masses, otherwise advection of oceanic air was observed (Figure 1).

2.2. Instrumentation

[9] A suite of online instruments was deployed to characterize the aerosol chemical composition and their physical properties [e.g., *Laborde et al*., 2012]. These included a high-resolution time-of-flight aerosol mass spectrometer (HR-ToF-AMS) as the main instrument of this paper (see section 2.2.1). In addition, online measurements of black carbon (BC) were performed using a seven-wavelength aethalometer (model AE31, Magee Scientific) and particle size distribution was measured by a SMPS (scanning mobility particle sizer) in the size range 10.6–495.8 nm.

[10] Instruments were connected to a common sampling line (built with 3/8 in. o.d. stainless steel tubing) fitted with a PM_{10} main inlet positioned outside the trailer at ~4 m above ground. The total sampling flow was 16.4 L min^{-1}. The AMS was connected to the main sampling line via a 6 mm o.d. stainless steel tube with a total flow rate of ~1 L min^{-1}. Prior to the AMS measurements, the aerosol was dried with two Nafion-dryers (SN ND07-43, SN ND07-45) with the relative humidity (RH) after the drying ranging between 27% and 57.6% (average value = 44%).

[11] The $PM_{2.5}$ filter samples (150 mm diameter quartz fiber filters, Tissuquartz®) were collected at 12 h intervals, using a high-volume sampler (Digitel, DA-80) for offline chemical speciation analyses. A 1 cm^2 filter punch was analyzed for elemental carbon (EC) and organic carbon (OC), using a Sunset Lab analyzer [*Birch and Cary*, 1996] and following the EUSAAR_2 protocol temperature program proposed by *Cavalli et al*. [2010]. Sample fractions of 11.34 cm^2 were extracted into 15 mL of ultrapure water by 30 min short vortex agitation to analyze ionic species including NH_4^+, NO_3^-, SO_4^{2-} and methanesulfonic acid (MSA). Ions were analyzed by ion chromatography and quantified based on the response factor of authentic standards, as described in *Jaffrezo et al*. [1998]. $PM_{2.5}$ chemical composition was also measured by a PILS-IC system (particle-into-liquid sampler-ion chromatograph), providing chromatograms to quantify the main inorganic species (Na^+, NH_4^+, K^+, Ca^{2+}, Mg^{2+}, Cl^-, NO_3^-, SO_4^{2-}) after growing the aerosols into droplets and collecting them by inertial impaction [*Sciare et al*., 2011].

2.2.1. HR-ToF-AMS

[12] A detailed description of the HR-ToF-AMS can be found elsewhere [*DeCarlo et al*., 2006] and the general working principle is also described in *Canagaratna et al*. [2007]. Briefly, air is sampled through a 100 μm critical orifice into an aerodynamic lens. The obtained particle beam is accelerated under vacuum conditions (10^{-5} Torr) into a sizing chamber, where the particles impact on a heated surface (600°C) and the non-refractory species vaporize. Here, electron ionization at 70 eV takes place on the resulting gas and the ions are extracted into the detection region to be classified by the mass spectrometer. The HR-ToF-AMS is characterized by having mass resolving power sufficient to distinguish individual ions at the same nominal *m/z* (within the mass range up to ~100 *m/z*) and two reflectron operational modes (V and W, where W mode utilizes a longer ion flight path in the mass spectrometer, thereby trading decreased signal for increased spectral resolution) as described in *DeCarlo et al*. [2006]. Measurement of the particle time-of-flight between a spinning chopper wheel at the lens exit and detection in the mass spectrometer yields size-dependent mass spectra.

[13] The HR-ToF-AMS was operated at SIRTA with an in-line thermodenuder (TD) to investigate the volatility of the non-refractory species measured by the AMS. The HR-ToF-AMS alternated between direct sampling of ambient air (AMB) and sampling through the thermodenuder (TD), while alternating between V and W modes in each configuration. This protocol yields four distinct operating modes: AMB_V, AMB_W, TD_V, and TD_W. Each mode had a sampling time of 2.5 min. The settings of the V-mode were 5 s in the mass spectrum (MS) mode (2.5 s chopper open and 2.5 s chopper closed) and 5 s in the particle time of flight (PToF) mode. Only MS mode was recorded in the W configuration (10 s in total, with the chopper for 5 s in the open position and 5 s in the closed one) due to the lower signal to noise. This work presents only data acquired during the AMB_V and the AMB_W configurations.

[14] The AMS data were analyzed using the SQUIRREL (SeQUential Igor data RetRiEvaL) v1.51 and PIKA (Peak Integration by Key Analysis) v1.10C, (D. Sueper, University of Colorado-Boulder, Boulder, CO, USA) for the IGOR Pro software package (Wavemetrics, Inc., Portland, OR, USA). Air interferences were removed by adjusting the fragmentation table [*Aiken et al*., 2008; *Allan et al*., 2004], and ionization efficiency and collection efficiency corrections were applied to the data set [*Canagaratna et al*., 2007]. Collection efficiency (CE) was calculated by (1) comparing the measured SMPS volume minus the BC volume to the estimated AMS volume, (2) AMS intercomparison experiments performed during the campaign [*Freutel et al*., 2013] where their CE was estimated with independent methods (e.g., SMPS volume comparison), and (3) filters comparisons. The AMS vs. SMPS minus BC volume comparison provided a slope of 0.38 ± 0.002, therefore a CE equal to 0.38 was assumed (see section SI-1.1 of the auxiliary material), in order to provide good agreement between our AMS measurements with external data, such as other AMS, filters, and PILS, as reported by *Freutel et al*. [2013].

[15] Default relative ionization efficiencies (RIE) were assumed for organics (1.3) and sulfates (1.2), while an RIE value of 3.3 was adopted for ammonium, based on ammonium nitrate calibrations conducted during the campaign. The comparison between the offline and AMS measurements for the organic carbon (OC) and for SO_4^{2-} is discussed in the auxiliary material (SI-1.2).

[16] High-resolution analysis [*DeCarlo et al*., 2006] was performed on each ion in the mass range 12–100 *m/z* with ion fitting applied separately to the open and closed spectra. The ions deriving from ambient aerosol were then calculated as the difference of open signal minus closed signal. Based on their elemental composition (content of C, O, H, N, S), ions were then grouped into chemical families: C_xH_y, $C_xH_yO_z$ ($z = 1$), $C_xH_yO_z$ ($z > 1$), $C_xH_yN_w$, and C_xS_j, where the indices x, y, z, w, j represent the number of C, H, O, N, S atoms, respectively. Elemental ratios of O : C, H : C, N : C, S : C, and the OM : OC (organic matter to organic carbon) ratio were also calculated as described by *Aiken et al*. [2007, 2008].

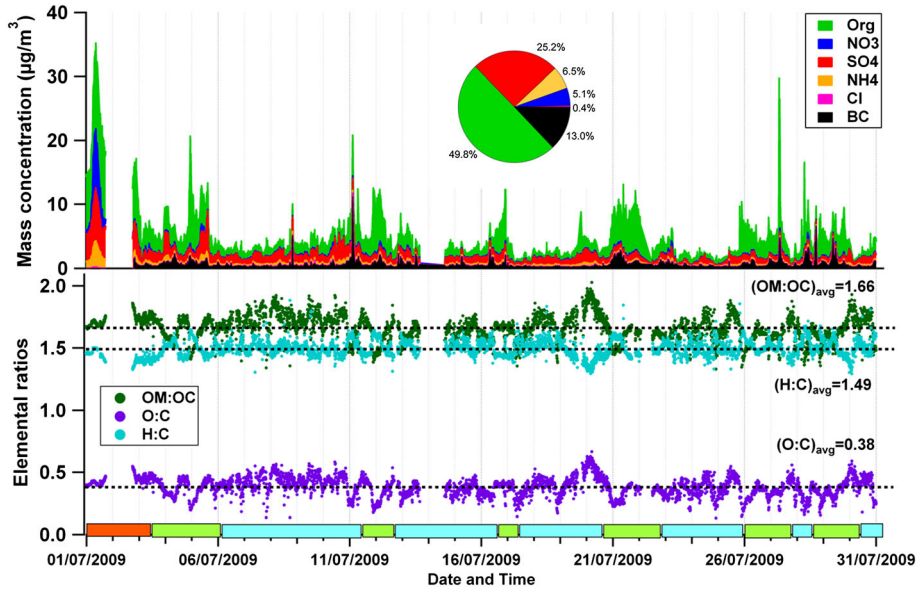

Figure 1. Temporal variation of AMS species (organics, sulfate, nitrate, ammonium and chloride), black carbon from aethalometer measurements (BC) and organic elemental ratios (OM : OC, O : C, H : C). The colors on the *x* axis represent the air masses classification (orange = continental, light blue = Atlantic clean, and light green = Atlantic polluted).

2.3. Source Apportionment

[17] The PMF analysis was applied to the high-mass resolution AMS organic mass spectra to describe different organic aerosol components in terms of their time series, mass spectra, and elemental ratios. PMF analyses were performed on three different inputs, as discussed in section 4.

[18] The PMF model is described by the following equation [*Paatero and Tapper*, 1994]:

$$X = \sum_{k=1}^{p} (G_{ik} \cdot F_{kj}) + E_{ij}$$

where X represents the matrix of the measured AMS organic mass spectra (in this case the time series of high-resolution MS from 12 to 100 *m/z*), *F* is the matrix of the factor profiles (organic sources), *G* the matrix of the temporal variability of each source, and *E* the residual matrix. The subscript *i* corresponds to time, *j* to *m/z*, and *k* to a discrete factor. The PMF model does not require any a priori assumption regarding the features of the source mass spectra or time series, except that *F* and *G* must be greater than 0 to be physically meaningful.

[19] The PMF algorithm iteratively minimizes the object function Q, defined as

$$Q = \sum_{i} \sum_{j} (E_{ij}/S_{ij})^2$$

where S_{ij} is the AMS measurement error, which includes electronic noise, ion-to-ion variability at the detector, and ion counting statistics [*Allan et al.*, 2003]. Recommendations for organic and uncertainty matrix preparation [*Ulbrich et al.*, 2009] were adopted as follows. A minimum counting error of 1 ion was applied to the measurements. Low signal-to-noise *m/z* values (SNR < 0.2) were removed, whereas "weak" variables (0.2 < SNR < 2) were downweighted by a factor of 2 [*Paatero and Hopke*, 2003]. The errors of masses 15.9949 (O^+), 17.0027 (OH^-), 18.0106 (H_2O^+), 27.9949 (CO^+), 43.9898 (CO_2^+) were increased to prevent overweighting of the organic contribution at *m/z* 43.9898 as these are calculated as constant ratios to the air-corrected signal at *m/z* 43.9898 [*Allan et al.*, 2004; *Ulbrich et al.*, 2009]. Isotopes were excluded from the HR-PMF calculations to reduce overweighting issues associated with some masses and due to their very low signal-to-noise ratios. The investigation of rotational ambiguity and local minima in the solutions is described in sections SI-2.3 and SI-2.4 of the auxiliary material.

[20] The analysis of aerosol sources was performed using the CU AMS PMF Execute Calcs Tool version 2.04 [*Ulbrich et al.*, 2009] as a front end for the PMF2 model [*Paatero*, 2007].

3. Aerosol Chemical Composition

[21] Over the whole campaign the concentration levels of submicron species were quite low (on average 4.5 $\mu g/m^3$; Figure 1) due to the influence of clean oceanic air masses. The aerosol was dominated by organic matter (49.8%) and sulfate (28.7%), while lower contributions were associated with black carbon (13%), nitrate (5.1%), ammonium (6.5%), and chloride (0.4%). The aerosol was not fully neutralized over the month of measurements (see also section SI-1.3 of the auxiliary material), having a $NH^+_{4\,measured}$ to $NH^+_{4\,neutral}$ ratio equal to 0.74 ± 0.001 (with an uncertainty of the relative ionization efficiency value for ammonium nitrate of 10%), where $NH^+_{4neutral}$ represents the amount of ammonium needed to neutralize the measured NO_3^-, SO_4^{2-} and Cl^-. The neutralization ratio was 0.83 ± 0.02 during the continental period at the beginning of the campaign

consistent with previous observations in marine-influenced regions [*Dall'Osto et al*., 2010; *Hildebrandt et al*., 2010].

[22] Figure 1 also shows the elemental ratios calculated from the high-resolution AMS data. These ratios reflect the degree of oxidation of the organic matter and can be used to probe the aging processes during atmospheric transport of particles emitted in different environments. The average OM : OC, O : C, and H : C ratios were equal to 1.66 ± 0.11, 0.38 ± 0.08, and 1.49 ± 0.07, respectively, consistent with previous ambient studies, where the O : C range for secondary OA is 0.27–0.43, and the H : C and OM : OC ratios vary from 1.41 to 1.89 and from 1.41 to 2.15, respectively [*Aiken et al*., 2008]. Table 1 summarizes the average PM_1 chemical composition and the organics' O : C, H : C, and OM : OC ratios for the three categories of air masses. During the continental event at the beginning of the campaign, much higher concentrations were measured both for organics ($7.17 \pm 3.39\ \mu g/m^3$) and secondary inorganic products ($SO_4^{2-} = 3.47 \pm 1.98\ \mu g/m^3$, $NO_3^- = 1.46 \pm 2.44\ \mu g/m^3$, and $NH_4^+ = 1.14 \pm 0.97\ \mu g/m^3$) compared with oceanic-influenced air masses (organics = 1.22–3.39 $\mu g/m^3$, $SO_4^{2-} = 1.05$–$1.11\ \mu g/m^3$, $NO_3^- = 0.14$–$0.21\ \mu g/m^3$, and $NH_4^+ = 0.26$–$0.28\ \mu g/m^3$). In relative terms, the fractional chemical composition measured by the AMS was also affected by air mass origin: organics contributed 54%, 45.3%, and 67.7% for continental, Atlantic clean, and polluted events, respectively; the corresponding sulfate fractions were 26.1%, 39.0%, and 22.1% and the nitrate ones 11.0%, 5.2%, and 4.3%. Slightly higher O : C and OM : OC ratios were also observed during the continental-influenced period.

[23] The median diurnal patterns of inorganic species such as SO_4^{2-} and NH_4^+ were rather flat, representing the influence of regional formation, while NO_3^- concentrations peaked during the morning rush hours due to the combination of multiple factors (e.g., temperature, boundary layer height, and emission trends). Daily patterns in the organic fraction are discussed in section 4.2, where their diurnal variability is explained in terms of local and regional organic emission sources. The diurnal patterns of the calculated elemental ratios are distinct for each ratio (Figure 2). Influenced by local primary emissions of non-oxidized matter (such as traffic), the H : C ratio increases during the morning traffic peak and the evening. In contrast, the O : C and OM : OC ratios increase during daytime due to photochemical SOA production and the smaller contributions from primary sources.

4. Aerosol Source Apportionment Results

[24] Three separate PMF analyses were performed: (1) PMF on unit mass OA spectra (UMR-PMF_{OA}); (2) PMF on high resolution OA spectra (HR-PMF_{OA}); and (3) PMF on high resolution OA and SO_4^{2-} spectra (HR-$PMF_{OA/SO4}$). For the three analyses, five-factor solutions were selected, including both primary and secondary organic aerosol sources. The primary OA factors were related to traffic (hydrocarbon-like OA, HOA) and cooking (COA) emissions. Two secondary OA factors were identified, associated with low volatility and semi-volatile oxidized aerosols (LV- and SV-OOA). The fifth factor was assigned to marine OA (MOA). In this section, we compare the output of the three analyses performed (section 4.1), attribute the PMF factors to their respective sources, and assess their chemical characteristics, variability, and contributions (section 4.2).

[25] The five-factor solution was selected based on the good interpretability of the identified sources (mass spectra and time series correlations with external data, diurnal variability of the sources, etc.). No additional information was retrieved from higher number factor solutions, where a mathematical recombination of the OOA-like and HOA factors was observed.

4.1. Validation of PMF Results

[26] A detailed comparison between the apportionment of UMR-PMF_{OA} and HR-PMF_{OA} is described in section SI-3 of the auxiliary material. Briefly, the two methods agree within 30% for the contributions of all five factors, showing similar time series ($R^2 > 0.71$) and similar mass spectra ($R^2 > 0.85$).

[27] To apportion sulfate sources, the high-resolution OA and SO_4^{2-} spectra were included together in a single matrix for PMF (HR-$PMF_{OA/SO4}$ data matrix). Because the time series and the profiles obtained from the HR-PMF_{OA} and HR-$PMF_{OA/SO4}$ are similar, we retain the same factor nomenclature (SV- and LV-OOA, MOA, HOA, and COA) despite the presence of sulfate ions in the latter factor mass spectra.

[28] A comparison between the PMF results of HR-PMF_{OA} and HR-$PMF_{OA/SO4}$ in terms of organic mass spectra, time series, and residuals is detailed in section SI-4 of the auxiliary information. First, it should be noted that the residual time series is not affected by including the sulfate ions (Figure SI-4.3). This indicates that the additional sulfate masses are well represented by the model because their residuals are negligible compared to those of the organics. *Chang et al*. [2011] already reported the use of combined inorganic and organic AMS spectra to improve PMF analysis. In order to better assess the impact of including the sulfate ions in PMF, a downweighting procedure was applied. Increasing the uncertainties associated with SO_4^{2-} ions by a factor of 10, the results are only slightly affected: the solution is characterized by stable source time series and mass spectra (Figures SI-4.4 and SI-4.5), meaning that the sulfate ions do not strongly pull the PMF solutions.

[29] The inclusion of sulfate peaks in PMF marginally influenced the apportionment and contribution of HOA and MOA (variation of 4% and 9%) and during specific events affected the cooking factor by up to 30%. The major difference between the solutions of the two PMF analyses is the reapportionment of *m/z* 44 between the two oxidized organic aerosol factors (LV-OOA and SV-OOA) and consequently the split between these two fractions and their OM : OC and O : C ratios. Adding the sulfates to the PMF calculation led to an increase of the fraction of *m/z* 44 in the LV-OOA such that this component would appear more oxidized (Figure SI-4.1). At the same time, the contribution of the LV-OOA was significantly reduced (up to 3.6 times lower), especially during the continental period that occurred in the beginning of the campaign and the events on 16–17 and 21 July (Figure SI-4.2). Conversely, adding the sulfates in the apportionment does not affect the specific diurnal patterns of the OOA fractions, meaning that although the split between the two OOA fractions is method dependent, their major features are always clearly identified. Hereafter

Table 1. Average Concentration ($\mu g/m^3$) ± Standard Deviation of the Aerosol Chemical Composition and Elemental Ratios From AMS and Aethalometer Data for Different Air Mass Types[a]

	Atlantic Clean	Atlantic Polluted	Continental	Whole Campaign
Org	1.22 ± 0.82	3.39 ± 2.06	7.17 ± 3.39	2.45 ± 2.33
NO_3	0.14 ± 0.12	0.21 ± 0.14	1.46 ± 2.44	0.26 ± 0.72
NH_4	0.26 ± 0.12	0.28 ± 0.17	1.14 ± 0.97	0.33 ± 0.36
SO_4	1.05 ± 0.49	1.11 ± 0.67	3.47 ± 1.98	1.23 ± 0.96
Cl	0.02 ± 0.03	0.01 ± 0.02	0.04 ± 0.05	0.02 ± 0.03
BC	0.50 ± 0.56	0.91 ± 0.71	0.61 ± 0.30	0.65 ± 0.62
PM_1	3.19 ± 1.60	5.92 ± 2.73	8.43 ± 4.44	4.47 ± 2.74
O : C	0.40 ± 0.08	0.36 ± 0.07	0.44 ± 0.04	0.38 ± 0.08
H : C	1.50 ± 0.07	1.50 ± 0.07	1.42 ± 0.04	1.49 ± 0.07
OM : OC	1.68 ± 0.11	1.62 ± 0.09	1.72 ± 0.04	1.66 ± 0.11

[a]PM_1 values represent the sum of AMS and BC measurements.

results from HR-PMF_{OA} and HR-$PMF_{OA/SO4}$ (without the sulfate downweight) will be used for the OA and SO_4^{2-} apportionment, respectively.

4.2. Primary and Secondary Aerosol Sources

[30] Figure 3 shows the organic aerosol mass spectra of the five deconvolved factors from the HR-PMF_{OA}. The factor spectra are colored based on chemical families, including $C_xH_y^+$, $C_xH_yO_z^+$ (z = 1), $C_xH_yO_z^+$ (z > 1), $C_xH_yN_w^+$, and $C_xS_j^+$, where the indices x, y, z, w, j represent the number of C, H, O, N, S atoms in each *m/z* fragment, respectively. These spectra are attributed to specific sources by comparing them with literature profiles (Figure SI-2.1). Table 2 reports specific organic ions identified as markers for each PMF component. The tracers were selected using two criteria: the contribution of an organic source to that ion is higher than 70% and the R^2 between the time series of that PMF factor and the considered ion is greater than 0.6. Note that for the SV- and LV-OOA, no specific marker was selected according to these criteria. The correlation of the time series of the factors with selected tracers (Figure 4) and the evaluation of their diurnal patterns (Figure 5) are used to support the attribution of the factors to the different sources.

4.2.1. Primary Emissions

[31] Traffic (HOA) and cooking emissions (COA) were identified as primary sources, averaging 12.0% and 14.7% of the total organic mass, respectively. HOA and COA mass spectra are dominated by the $C_xH_y^+$ family, resulting in high H : C ratios (range 1.74–1.84). The OM : OC ratios ranged between 1.32 and 1.38 while the O : C ratio varied between 0.13 and 0.16 (Figure 3), consistent with previous studies [*Aiken et al*., 2009; *Chirico et al*., 2010; *Mohr et al*., 2012]. An important distinction between the COA and HOA spectra is the presence of more highly oxygenated fragments at the same nominal *m/z* in COA [*Allan et al*., 2010; *Ge et al*., 2012; *He et al*., 2010; *Mohr et al*., 2012; *Sun et al*., 2011]. The COA mass spectrum shows an influence of wood burning-related ions, such as $C_2H_4O_2$ at *m/z* 60 (0.0069) and $C_3H_5O_2^+$ at *m/z* 73 (0.0063) [*Alfarra et al*., 2007]. These ions are known to be produced in biomass burning through the thermal breakdown of plant matter and it is therefore possible that they could also be produced by vegetable cooking. The correlation between the cooking time series with the total temporal variation of the ions $C_2H_4O_2^+$ and $C_3H_5O_2^+$ (R^2 = 0.49 and 0.5) suggests the possibility of outdoor barbecuing emissions contributing to this factor.

[32] During the measurement period, HOA shows a reasonable correlation with black carbon (BC) (R^2 = 0.48; Figure 4); the diurnal patterns of both species exhibit strong morning and evening peaks corresponding to increased traffic during rush hours (Figure 5). These trends are consistent with the increase (decrease) of H : C (O : C) ratios during the corresponding periods (Figure 2). A good tracer for cooking emissions was identified in the ion $C_6H_{10}O^+$ due to its high correlation with the COA time series (R^2 = 0.76), consistent with *Sun et al*. [2011]. COA peaks during the noon and evening meal hours, contributing up to 15.6% and 27.3% of OA, respectively. These specific daily patterns of HOA and COA are consistent with their emission processes and the evolution of the mixing layer height and strongly suggest a rather local origin for the traffic and cooking sources during the study.

4.2.2. Oxygenated Organic Aerosol

[33] Oxygenated OA included low volatility (LV-OOA, 25.2% of total OA) and semi-volatile (SV-OOA, 32.4% of OA) factors, similar to previous summertime studies [*DeCarlo et al*., 2010; *Lanz et al*., 2007; *Ulbrich et al*., 2009; *Zhang et al*., 2005]. They are characterized by high O : C ratios (O : C = 0.39 and O : C = 0.73 for SV- and LV-OOA, respectively) and low H : C ratios compared with fresh primary emissions (1.33–1.52; Figure 3). The aggregate OOA constituted approximately 58% of the total OA during the study.

[34] The LV-OOA correlated well with sulfate (R^2 = 0.64) and was likely influenced by regional processes, evidenced by the lack of distinct daily patterns for both species. The HR-$PMF_{OA/SO4}$ analysis indicated that on average a significant fraction of the AMS SO_4^{2-} was associated with the LV-OOA fraction (~49% or 0.59 $\mu g/m^3$).

[35] A very low correlation was observed between SV-OOA and nitrate (R^2 = 0.28), despite the expected influence of temperature on the gas/particle partitioning of both species. This observation is explained by their different diurnal patterns (Figure 5). SV-OOA showed a complex pattern with peaks at 4:00 and 18:00, and minima at 10:00 and midnight. The daytime maximum was likely due to local photochemical production of SOA from gaseous precursors and its condensation on pre-existing particles as observed by

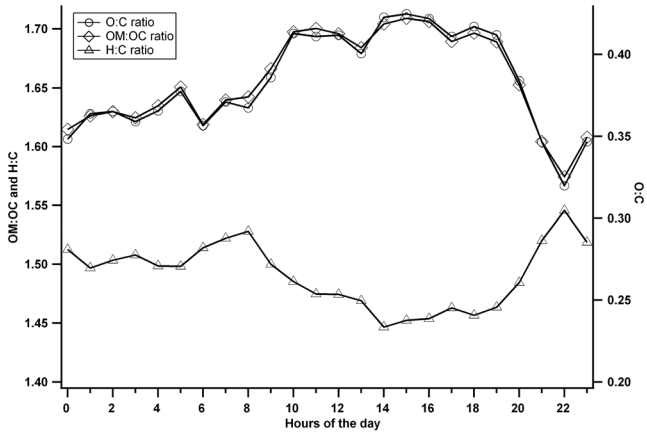

Figure 2. Diurnal patterns of median elemental ratios (OM : OC, O : C, H : C).

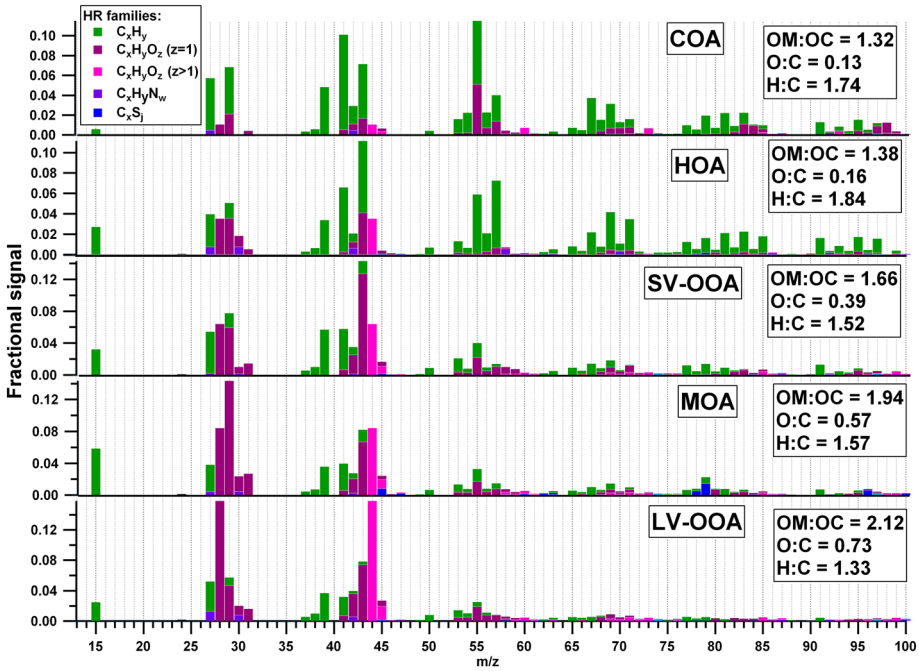

Figure 3. Mass spectra of the organic components separated by HR-PMF_{OA}.

Freutel *et al*. [2013]. In contrast, the morning peak could be due to the partitioning of semi-volatile species into the particle phase due to the lower temperature and higher relative humidity. However, the interpretation of this complex diurnal pattern is uncertain due to possible effects from other factors such as the low boundary layer height, lack of vertical dilution, and nighttime oxidation reactions by ozone or nitrate radicals. The SV-OOA concentrations started decreasing at 4 A.M. while the minimum of the temperature was reached only at 6 A.M. This shift between the maximum SV-OOA concentration and the minimum temperature could be explained by a change in the type of air masses, amount of water (RH dependency), and/or dilution. The temperature increase after sunrise caused partitioning to the gas phase of the most volatile species as well as dilution due to the rising boundary layer, both of which could affect the decrease of SV-OOA concentrations. During nighttime, both nitrate and SV-OOA increased due to condensation, but an anti-correlation was observed during daytime when NO_3^- evaporated into the gas phase, while SV-OOA increased by photochemical production. The diurnal variability of SV-OOA was independent of the synoptic wind regimes previously defined, again indicating that the SV-OOA fraction relates to locally formed SOA.

Table 2. Organic Markers for Each PMF Component[a]

Ion	Exact Mass	PMF Component	Fraction Explained by a Source	R^2
C_5H_{11}	**71.0861**	**HOA**	71.9%	0.79
C_5H_{12}	**72.0939**	**HOA**	73.3%	0.68
CH_2SO_2	**77.9775**	**MOA**	80.6%	0.66
CH_3SO_2	**78.9854**	**MOA**	80.5%	0.69
C_6H_{12}	**84.0939**	**HOA**	75.0%	0.79
C_6H_{13}	**85.1017**	**HOA**	74.6%	0.82
CH_4SO_3	**95.9881**	**MOA**	88.7%	0.82
C_7H_{13}	**97.1017**	**HOA**	75.6%	0.82
$C_6H_{10}O$	**98.0732**	**COA**	86.7%	0.76
$C_6H_{11}O$	**99.081**	**COA**	71.9%	0.63
C_7H_{15}	**99.1174**	**HOA**	82.8%	0.79

[a]Note that no unique marker was identified for SV- and LV-OOA.

4.2.3. Marine Emissions

4.2.3.1. Evidence of Marine Emissions Impact

[36] The last factor from the HR-PMF_{OA} analysis was assigned to marine emissions (MOA, 15.7% of OA) based on the following evidence: The presence of high levels of organic sulfur species in the factor mass spectrum suggests a marine origin. MOA was characterized by an average S : C ratio of 0.013 which is at least an order of magnitude higher than the S : C ratios of the other factors. The main ions contributing to the $C_xS_j^+$ family include CHS^+ ($m/z = 44.9799$), CH_3S^+ ($m/z = 46.9955$), $CH_2SO_2^+$ ($m/z = 77.9775$), $CH_3SO_2^+$ ($m/z = 78.9854$), and $CH_4SO_3^+$ ($m/z = 95.9881$). A similar marine factor was identified by *Chang et al*. [2011] within the ASCOS project (Arctic Summer Cloud Ocean Study) including both sulfate ions (*m/z* 48, 64, 80, 81, and 98) and *m/z* likely to contain organic sulfur species (*m/z* 79 and 96). The MOA time series also suggests a marine origin, as evidenced by its strong correlation with $PM_{2.5}$ filter measurements of MSA ($R^2 = 0.84$; Figure 6).

[37] Although sulfate and organic MOA can comprise a mixture of primary and secondary particles from anthropogenic (i.e., ship emissions) and biogenic marine emissions, ^{14}C measurements performed during the campaign suggest that this organic fraction is dominated by biogenic emissions, since the total oxygenated OA fraction accounts for ~90% of non-fossil origin (Beekmann et al., submitted manuscript, 2013). However, contribution of ship emissions to the SO_4^{2-} fraction cannot be excluded. First, in addition to $C_xS_j^+$ fragments, the MOA mass spectrum is characterized by oxygenated components and by the absence of hydrocarbon-like *m/z* (e.g., $C_4H_7^+$ and $C_4H_9^+$), resulting in a high O : C ratio of 0.57 (OM : OC = 1.94). These features suggest a possible

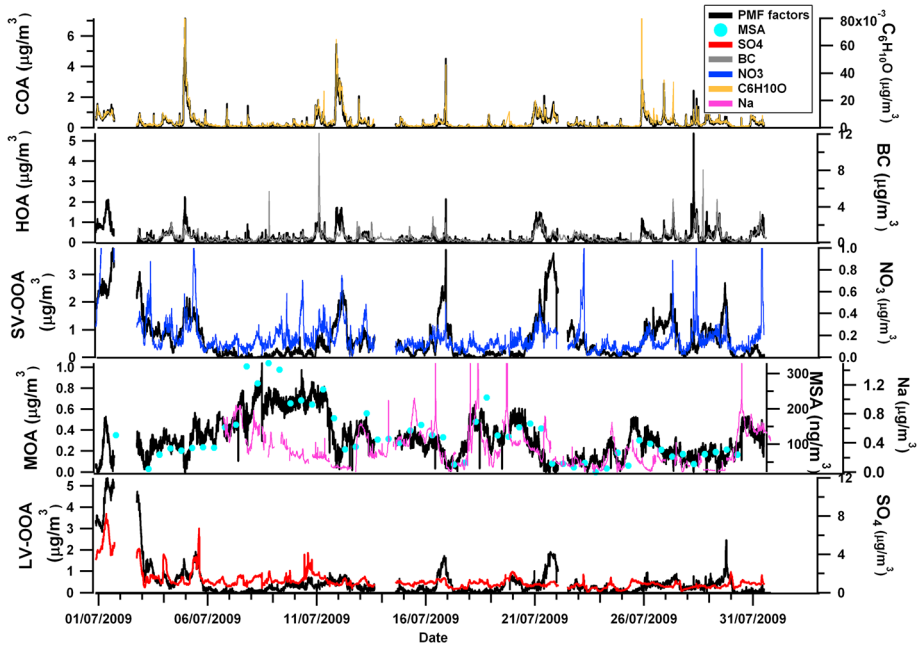

Figure 4. Time series of the identified organic factors from HR-PMF$_{OA}$ and correlations with ancillary data.

secondary origin of this factor (supported also by the strong correlation with MSA and marine sulfate), although a mixture with resuspended oxidized primary organic material from the ocean such as polyols and saccharides [*Decesari et al*., 2011] cannot be excluded. Further evidence for a biogenic source is the very low correlation of MOA with vanadium and nickel, unique tracers of primary ship emissions [*Viana et al*., 2009]. These elements also exhibit lower concentrations (0.78 ± 0.86 ng/m^3 and 3.96 ± 4.31 ng/m^3 for V and Ni, respectively) than would be expected if the air mass was strongly influenced by ship emissions.

[38] Finally, the strong correlation of MOA with MSA discussed above suggests a biogenic influence. Taken together, these observations strongly suggest that MOA observed here arises principally from biogenic precursors and is not strongly influenced by ship emissions. This explanation is consistent with ^{14}C measurements conducted over the Atlantic Ocean, indicating an overwhelming contribution of non-fossil carbonaceous aerosol [*Ceburnis et al*., 2011].

4.2.3.2. MOA Characteristics

[39] Similarly to SO_4^{2-} and LV-OOA, MOA does not exhibit any particular diurnal cycle, consistent with the

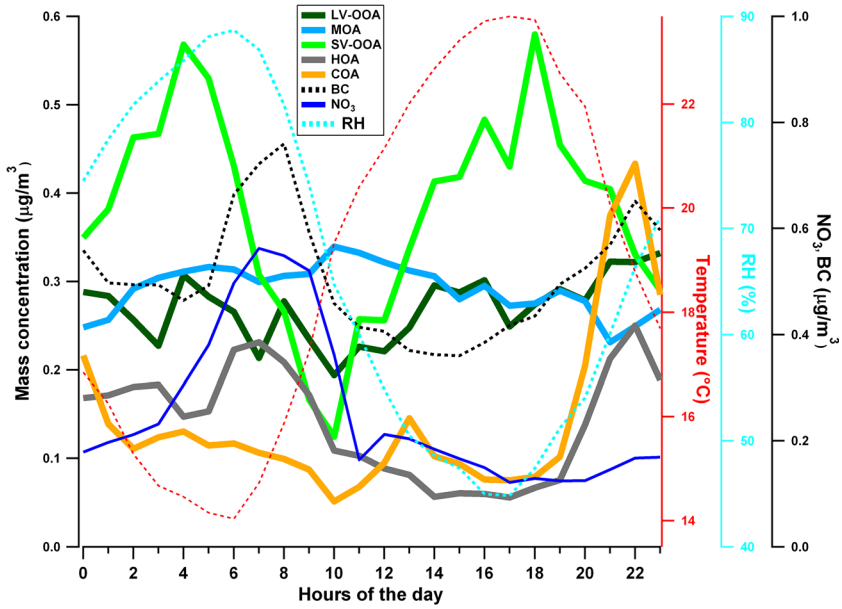

Figure 5. Diurnal variation of HR-PMF$_{OA}$ factors and their relative contribution to the total organic mass. Median values are reported for each source and species. For comparison, BC, NO_3^-, temperature, and relative humidity diurnal variations are shown.

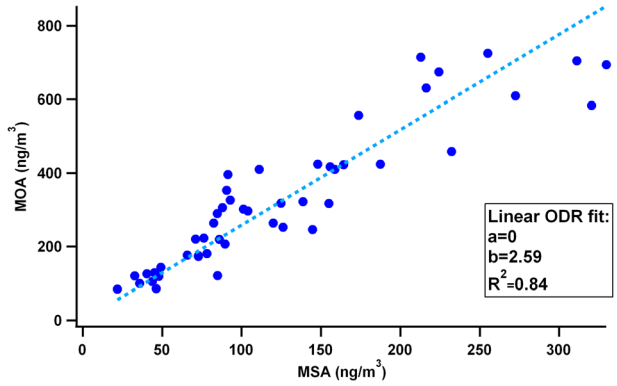

Figure 6. Scatter plot showing the correlation between MOA (from HR-PMF$_{OA}$) and MSA (from $PM_{2.5}$ filters).

regional origin of this fraction. During the period of study, MOA constitutes an important source, providing on average $0.23 \pm 0.14\ \mu g/m^3$ (15.7%) of OA and $0.59 \pm 0.89\ \mu g/m^3$ of SO_4^{2-} and accounting for about 41.4% of the sulfate detected by the AMS. AMS sulfate represents only non-sea-salt sulfate. Sea-salt sulfate is mostly undetected by the AMS because it is less likely to vaporize and occurs mostly in super micron particles [*Phinney et al.*, 2006], although recent AMS measurements evidenced the possibility to detect sea salt [*Ovadnevaite et al.*, 2012]. However, the $PM_{2.5}$ sea-salt sulfate can be estimated from filter measurements of $PM_{2.5}$ Na^+ and the mass ratio SO_4^{2-} to Na^+ in sea water (0.25) [*Sciare et al.*, 2003]. The estimated ss-SO_4^{2-} fraction contributes on average only $0.038 \pm 0.025\ \mu g/m^3$, significantly lower than the marine nss-SO_4^{2-}.

[40] Likewise, the contribution of the total sea salt to $PM_{2.5}$ can be estimated from the concentrations of $PM_{2.5}$ Na and the ratio of sea salt/Na (2.54) [*Bates et al.*, 2001]. Sea salt occurred mostly in the $PM_{2.5}$–PM_1 range and contributed $0.39 \pm 0.25\ \mu g/m^3$, consistent with previous measurements during periods of high marine biological activity. From the PMF results and filter-based apportionment, a chemical mass balance of the marine aerosol can be established. The marine aerosol thus consisted of an organic fraction ($0.23 \pm 0.14\ \mu g/m^3$), marine non-sea-salt sulfate ($0.59 \pm 0.89\ \mu g/m^3$) and $PM_{2.5}$ sea salt ($0.39 \pm 0.25\ \mu g/m^3$). *Dall'Osto et al.* [2010] observed, at the Mace Head Atmospheric Research Station located on the west Irish coastline, AMS organic concentrations to range between $0.02 \pm 0.01\ \mu g/m^3$ and $1.75 \pm 0.44\ \mu g/m^3$ and the sulfate ones between $0.67 \pm 0.17\ \mu g/m^3$ and $1.81 \pm 0.45\ \mu g/m^3$ depending on the origin of marine air masses. A salient element of this estimated mass balance is the high contribution of the organic matter in the processed marine air masses, which occur at the measurement site at similar concentrations as SO_4^{2-} (MOA/ $SO_{4\,marine}^{2-}$ on average equal to 1.01, 0.94, and 1.4 for the Atlantic clean, polluted, and continental periods, respectively).

4.2.3.3. MSA Estimation Using AMS Measurements

[41] Filter measurements indicate that a significant fraction of $PM_{2.5}$ marine SOA occurs as MSA, with levels measured on $PM_{2.5}$ filters ranging between 22 and 330 ng/m^3 (average of 122 ± 76 ng/m^3). *Phinney et al.* [2006] reported MSA values over the sub-arctic northeast Pacific equal to 167 ± 50 ng/m^3, while lower values are reported by *Chang et al.* [2012] for polar regions (10–80 ng/m^3). At Mace Head, measured MSA levels during marine-influenced air masses varied between 50 ± 10 ng/m^3 and 280 ± 70 ng/m^3 [*Dall'Osto et al.*, 2010] similarly to our observations.

[42] It is possible to estimate the PM_1 MSA levels in MOA using AMS measurements and the MSA fragmentation patterns reported by *Phinney et al.* [2006] and *Zorn et al.* [2008]. *Zorn et al.* [2008] measured the MSA fragmentation pattern at several AMS vaporizer temperatures; the standard vaporizer temperature of 600°C is used herein. MSA (parent ion $CH_3SO_3H^+$, $m/z = 96$) fragments mainly not only to m/z 15 (CH_3^+ ion) and to m/z 79 (ion $CH_3SO_2^+$), but also to the sulfate ions (ion SO^+, $m/z = 47.967$; ion SO_2^+, $m/z = 63.9619$). As one of the predominant and distinctive peaks of MSA, m/z 79 was chosen as the characteristic fragment for the MSA estimation [*Zorn et al.*, 2008]. The ratio between the relative contribution of the ion $CH_3SO_2^+$ (m/z 79) and the signal of the normalized reference spectra at m/z 79 was calculated to be equal to 0.22 and 0.16 in the case of Phinney and Zorn spectra, respectively [*Phinney et al.*, 2006; *Zorn et al.*, 2008]. The identified scaling factor was applied to derive the contribution of MSA to MOA mass spectrum and to the MOA time series to quantify the MSA mass (see Figure 7). Depending on the considered reference MSA mass spectrum [*Phinney et al.*, 2006; *Zorn et al.*, 2008], the estimated MSA concentration can represent on average $74.1\% \pm 20.31\%$ and $47.6\% \pm 13.1\%$ of the corresponding filter measurements.

[43] *Ge et al.* [2012] estimated the MSA mass (mMSA) with the following equation:

$$\mathrm{mMSA} = \frac{m\mathrm{CH_2SO_2} + m\mathrm{CH_3SO_2} + m\mathrm{CH_4SO_3}}{0.147}$$

where $m\mathrm{CH_2SO_2}$, $m\mathrm{CH_3SO_2}$ and $m\mathrm{CH_4SO_3}$ were the signal intensities of these three ions measured in ambient aerosols (in $\mu g/m^3$) and 0.147 their fractional contribution to the total signal in the HR-ToF-AMS spectrum of pure MSA. Application of this method to the current dataset yields MSA concentrations corresponding to $63 \pm 20.5\%$ of the MSA filter measurements, comparable to the previously discussed estimates.

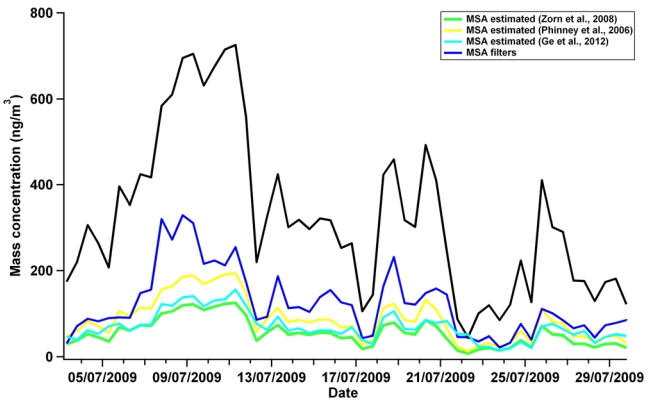

Figure 7. Time series comparison of total MOA, $PM_{2.5}$ MSA and estimated MSA from AMS measurements, based on *Phinney et al.* [2006] and *Zorn et al.* [2008] MSA fragmentation pattern and *Ge et al.* [2012] approach.

[44] It is important to note that the ratio between the measured (filter-based) and estimated (AMS-based) MSA concentrations is not constant. Therefore, the discrepancy observed between the two techniques is not caused by a constant bias related to the estimation technique. One parameter impacting this estimation is the different size cut-off between the AMS (PM_1) and the filters ($PM_{2.5}$). Although MSA derives from secondary formation processes [*Gondwe et al*., 2004; *O'Dowd et al*., 2004], it is often found in the super micron range, beyond the AMS transmission window [*Cavalli et al*., 2004; *Pszenny*, 1992; *Virkkula et al*., 2006]. In addition some MSA and MOA events correlate well with the Na concentrations, meaning that MSA could be condensed onto sea-salt particles (the fraction of MSA in the coarse mode depends on the ratio of the condensational sink in the coarse and fine mode), which are not quantitatively detected by the AMS due to their larger size [*Phinney et al*., 2006] and refractory behavior.

[45] Moreover, the contribution of $CH_3SO_2^+$ to mass 79 varies as a function of heater temperature (0.077 at 700°C, to 0.11 at 500°C) [*Zorn et al*., 2008], introducing an additional uncertainty of up to 30% in the MSA mass calculation. Finally, additional uncertainty is associated with the assumption of the relative ionization efficiency of MSA, measured by *Phinney et al*. [2006] to be equal to 1.15 and estimated by *Zorn et al*. [2008] from the organic (1.4) and sulfate (1.2) RIEs to be 1.3. In our case, the assumed RIE is equal to 1.3 when considering the *Zorn et al*. [2008] fragmentation pattern and 1.15 for the one of *Phinney et al*. [2006], since no MSA calibration was performed. Therefore, our MSA estimation can most probably be considered as an approximation of the fraction of MSA in the PM_1 range. In future studies, for sites that could be exposed to the influence of marine air masses, an AMS MSA calibration is recommended in order to determine the relative ionization efficiency of MSA and improve the MSA quantification using AMS measurements. Moreover, *Zorn et al*. [2008] noted that MSA evaporates under normal room conditions, so one would need to use the AMS vacuum aerodynamic diameter (D_{va}) to get size information (as opposed to, e.g., take the mobility diameter from a size selection by a differential mobility analyzer).

[46] Based on our calculation, PM_1 MSA contributes ~20% (from 17.2% up to 26.8% depending on the adopted estimation approach) to the marine OA, consistent with previous coastal measurements (*Rinaldi et al*., 2010 and references therein), with the remaining ~80% of MOA consisting of an unidentified complex mixture of oxygenated organic compounds. Another useful piece of information retrieved from this analysis is the MSA/nss-SO_4^{2-} ratio in the marine aerosol, where the marine nss-SO_4^{2-} is obtained from the HR-$PMF_{OA/SO4}$. Such a ratio is reported to vary in the super-micron range between 0.1 and 0.4 depending on latitude and temperature (0.4 for polar regions and 0.1 for tropical and midlatitude areas) [*Gondwe et al*., 2004]. The MSA_{PM1}/nss-SO_4^{2-} (based on AMS estimated MSA) and $MSA_{PM2.5}$/nss-SO_4^{2-} (based on filter measured MSA) are 0.10 ± 0.07 and 0.26 ± 0.07, respectively, consistent with literature values, Paris latitude, and air mass origin [*Gondwe et al*., 2004]. Finally, when considering the total nss-SO_4^{2-} measured by the filters, the $MSA_{PM2.5}$/nss-SO_4^{2-} ratio is lower (0.12 ± 0.06), as the sulfate arises from both marine and continental sources. As a result, this ratio is highly dependent on the air mass origin: During Atlantic clean events, it is on average equal to 0.149 ± 0.053, whereas much lower ratios are observed for the continental and somewhat lower for Atlantic polluted episodes (ratio equal to 0.028 ± 0.015 and 0.090 ± 0.035, respectively).

5. Impact of Air Mass Origin on Aerosol Composition

[47] This section addresses the local versus regional origin of the sources identified in the previous sections, and whether these source contributions occur with a specific directionality. The discussion of local/regional/directional influences is particularly appropriate for the case of Paris, given its status as a post-industrial megacity [*Crippa et al*., 2013].

[48] The relationship between air mass origin and PMF factor contributions provides insights in aerosol sources, distinguishing between local and regional emissions. Figure 8 shows rose plots of OA, NO_3^-, SO_4^{2-}, BC, and the OA components identified using PMF. OA components are colored by their contributions to the total organic mass, while other species are colored by their contribution to the total PM_1 (sum of the AMS and the aethalometer mass). Wind data were recorded at SIRTA using a permanent SODAR system at an altitude of 100 m [*Haeffelin et al*., 2005]. The comparison of the wind vertical profiles at SIRTA and over the whole Parisian region showed uniform distribution throughout the area. This suggests that local wind measurements are representative of the regional air masses direction. A summary of the average organic and sulfate source contributions for the different air mass classes (continental, Atlantic clean, and Atlantic polluted) is presented in Figure 9.

[49] The PM_1 concentrations were higher during continental events when the site was influenced by winds mainly coming from the northern sector (Figure 8a), whereas Atlantic clean and polluted periods were characterized by lower concentrations. PM_1 concentrations during these periods were on average equal to $3.2 \pm 1.6\ \mu g/m^3$ (Atlantic clean), $5.9 \pm 2.7\ \mu g/m^3$ (Atlantic polluted), and $8.4 \pm 4.4\ \mu g/m^3$ (continental). Also the PM_1 chemical composition was strongly affected by the air mass origin. Continental air masses were dominated by the inorganic fraction, with NO_3^- and SO_4^{2-} accounting on average for 10.5% and 25% ($1.5\ \mu g/m^3$ and $3.5\ \mu g/m^3$), respectively. By contrast, marine air masses contained very low contributions of nitrate to the total PM_1 (4.4% or $0.14\ \mu g/m^3$ during the clean marine periods), with sulfate and OA contributing on average 32.9% ($1.05\ \mu g/m^3$) and 38.2% ($1.22\ \mu g/m^3$), respectively. Unlike the nitrate, the levels of OA are not highly affected by the wind direction, as this fraction derives from several different local and regional sources.

[50] The LV-OOA and MOA components are strongly impacted by air mass origin (Figure 8b), consistent with the regional character indicated by their diurnal patterns (Figure 5). MOA dominated when the site was downwind of the Atlantic Ocean (Western direction), whereas LV-OOA was greater during the continental pollution events (up to four times higher than during the Atlantic-influenced periods; see Figure SI-6). Figure 9 shows that during continental events OA was dominated by both OOA fractions

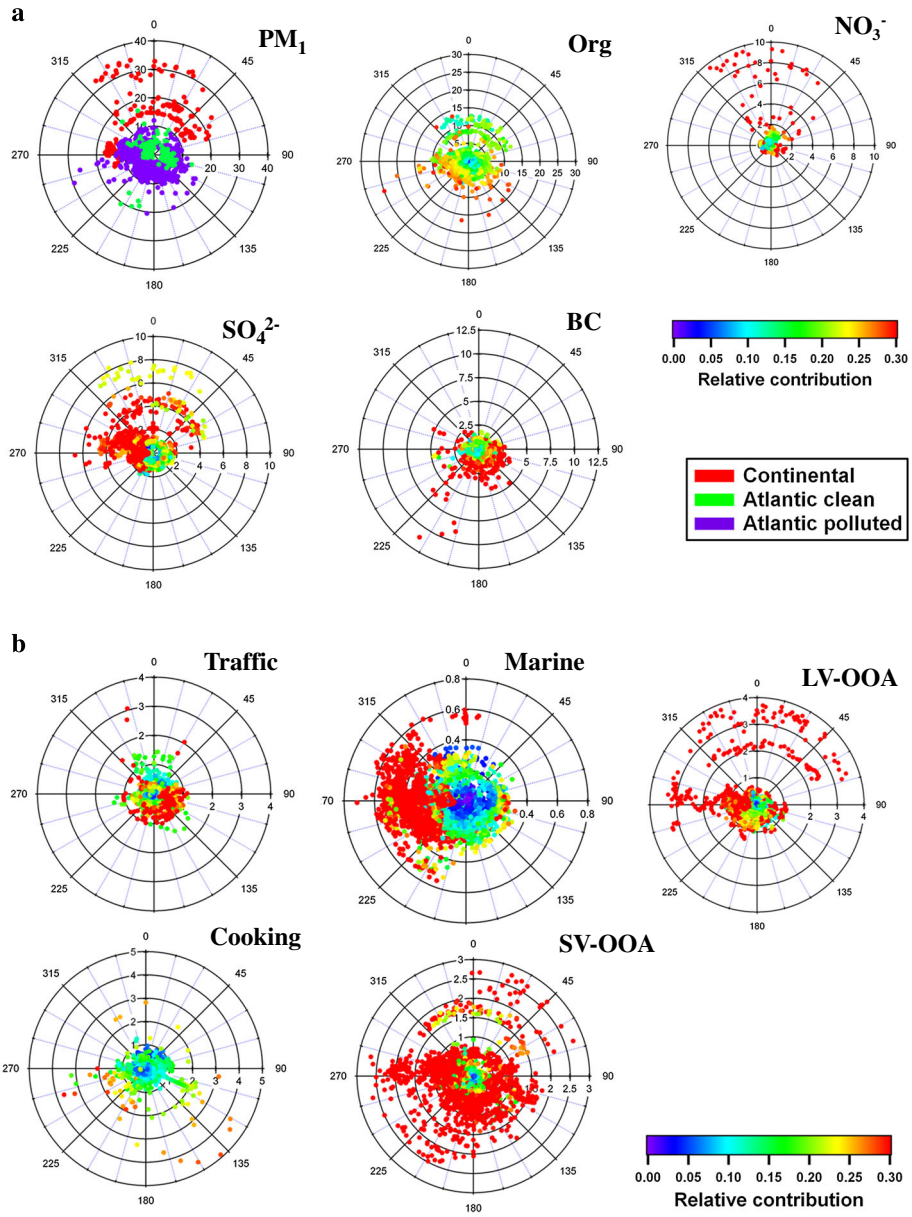

Figure 8. (a) Wind roses of the PM_1 components (total PM_1, organic, nitrates, sulfates and black carbon). The radial axes represent the absolute concentration in $\mu g/m^3$ of each component, while the color scale denotes the relative contribution of each component to the total PM_1 mass. The air mass classification (continental, Atlantic clean and polluted) is referred to the total PM_1 wind rose case. (b) Wind roses of the PM_1 organic components (HOA, COA, MOA, SV-OOA and LV-OOA). The radial axes represent the absolute concentration in $\mu g/m^3$ of each component, while the color scale denotes the relative contribution of each OA component to the total organic mass.

(LV-OOA = 47% or 3.7 $\mu g/m^3$ and SV-OOA = 34% or 2.7 $\mu g/m^3$), while only a minor part was associated with marine emissions (MOA = 3% or 0.2 $\mu g/m^3$). In contrast, during the clean marine events, MOA was significant (38% or 0.51 $\mu g/m^3$), whereas the fraction of the OOA factors was lower (LV-OOA = 17% or 0.23 $\mu g/m^3$ and SV-OOA = 19% or 0.25 $\mu g/m^3$). Local, continental, and marine emissions all influence the aerosol during the Atlantic polluted periods, with the OA composed of 50% OOA (2.17 $\mu g/m^3$), 9% MOA (0.33 $\mu g/m^3$), and 41% primary emissions (1.13 $\mu g/m^3$). SV-OOA, mostly attributed to local SOA production, exhibits a homogeneous distribution over the whole range of wind directions. Although nighttime SV-OOA formation appears not to have any directionality since probably associated with the combined role of partitioning due to temperature and humidity effects and boundary layer evolution, the afternoon SV-OOA production seems to be influenced by winds coming from the 135°-315° sector and is possibly associated with local photochemistry. On the contrary, primary aerosol components are dominated by local cooking and traffic emissions. These represent a minor fraction of PM_1 (HOA = 8–15% of OA, COA = 8–12% of OA; Figure 9), independent of wind regime. HOA and BC contributions are higher for south-east winds, corresponding to the direction of

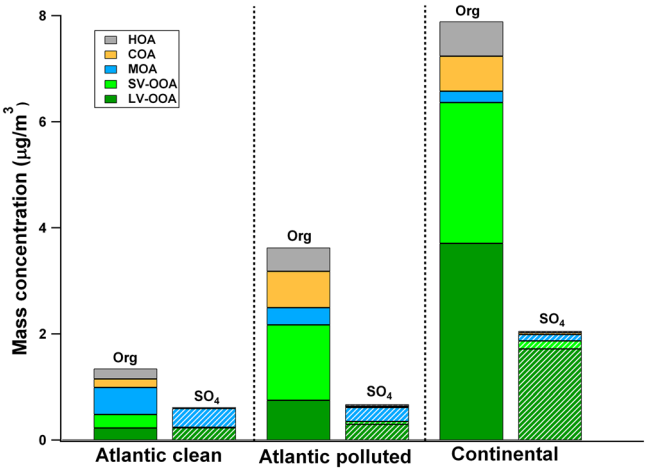

Figure 9. Organic and SO_4^{2-} source apportionment for the Atlantic clean, Atlantic polluted, and continental air masses. Solid colors represent the organic source apportionment obtained from the HR-PMF_{OA}; hatched colors denote the SO_4^{2-} apportionment derived from the HR-$PMF_{OA/SO4}$.

a major highway. Cooking emissions were not associated with any particular wind direction, indicating that they are not affected by a specific source region or by a point source contaminating our measurements (e.g., emissions of a restaurant), but are rather related to a diffuse source with an increasing input during lunch and dinner hours (see Figure 5).

[51] The PMF source apportionment of sulfate (HR-$PMF_{OA/SO4}$) supports its high abundance in both continental and marine events. The HR-$PMF_{OA/SO4}$ assigned the SO_4^{2-} to both the LV-OOA component, a continental long-range transported SOA, and to the marine emissions, MOA (their relative contribution is on average 38.5% and 47.5%, respectively; see SI-5). When the site was impacted by marine air masses, 39–58% of the SO_4^{2-} could be apportioned to MOA, while for continental events SO_4^{2-} was mainly associated with the LV-OOA fraction (84%). Due to the fragmentation of MSA to SO^+ and SO_2^+ ions, a small fraction of the SO_4^{2-} associated with MOA could be actually formed by MSA (~1.5 ng/m^3).

6. Summary on the PM_1 Source Apportionment and Conclusions

[52] The main findings of this work are summarized in Figure 10, where the PM_1 chemical composition derived from AMS-aethalometer measurements and the organic and sulfate source apportionment are represented. The aggregate primary emissions accounted for 26.3% of the total PM_1, including mostly traffic emissions (BC = 13% and HOA = 6%) and a contribution from cooking activities (COA = 7.3%). The aerosol is hence dominated by secondary compounds including inorganic (NH_4^+, SO_4^{2-}, and NO_3^-) and organic components (SV-OOA, LV-OOA, and MOA). The PMF analysis distinguishes between continental and oceanic sources, although some of the fractions apportioned, notably the LV-OOA_{OA} and the LV-OOA_{SO4}, might arise from both. The continental secondary aerosol consists of NO_3^-, a fraction of nss-SO_4^{2-} and both OOA fractions (dark and light green colors for LV-OOA and SV-OOA in Figure 10, respectively), totaling 65.9% of the total PM_1.

[53] Marine aerosol includes both OA (MOA PMF factor, 10.1% of PM_1 mass) and some SO_4^{2-} (13.6% of PM_1 mass), totaling 24% of PM_1. It should be noted, however, that this may be an underestimate of total PM_1 because sea salt is excluded. Additionally, LV-OOA_{OA} and the LV-OOA_{SO4} are assumed to be of continental origin, while in reality marine sources may also contribute. Although Atlantic Ocean air masses have been previously observed to result in reduced PM and VOC concentrations in Paris [*Gros et al*., 2011; *Sciare et al*., 2010], here it was possible for the first time to quantify this reduction and its effect on PM composition by combining PMF modeling and air mass analysis. Surprisingly for a heavily urbanized, inland megacity such as Paris (~200 km from the ocean), biogenic marine emissions still contribute significantly to SO_4^{2-} and OA levels, representing up to 23.7% of the total PM_1 mass. These results are consistent with the findings of *Sciare et al*. [2010], showing the influence of air mass origin on the aerosol concentration and composition in the Paris area.

[54] This result supports the emerging picture that the primary emissions from the Paris megacity do not significantly influence regional air quality. On the contrary, regional aerosol sources have generally larger effects on Paris air quality than emissions from the metropolitan Paris itself. Similar conclusions were already drawn not only for smaller cities like Zurich in Switzerland [*Lanz et al*., 2010; *Mohr et al*., 2011], but also for other European megacities [*Harrison et al*., 2012]. These results are consistent with other studies performed in the context of the MEGAPOLI project [*Crippa et al*., 2013; *Freutel et al*., 2013], which also show a regional behavior of the aerosol and gas-phase pollutants over the Paris conurbation due to meteorological effects and the rather uniform distribution of emission sources. Therefore, the findings of our study not only relate to the background site where the measurements were performed, but are also likely representative of the entire Paris metropolitan area during the time frame of our study.

[55] During the MEGAPOLI 2010 winter campaign, similar organic aerosol sources were identified for the SIRTA site [*Crippa et al*., 2013], with cooking, HOA, biomass burning (typical of wintertime emissions), and oxidized

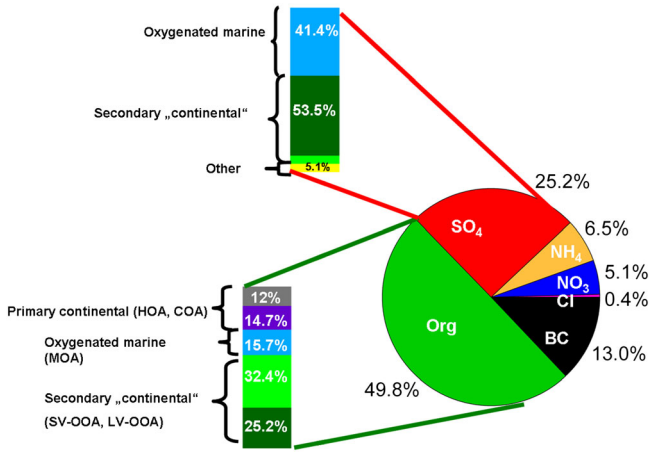

Figure 10. PM_1 mass balance, organics, and sulfate source apportionment. Note that LV- and SV-OOA (dark and light green, respectively) are assumed to be secondary continental sources, while in reality these factors may also be influenced by marine sources. The fraction "other" accounts for the primary source contributions to sulfate which are most probably mathematical artifacts.

OA factors identified by PMF. However, an important difference is that no marine source was identified in the winter measurements. This is likely due to several concurrent factors. First, secondary marine aerosol (such as MSA) is strongly dependent on temperature (maximum production in spring and summer) due to higher marine biological activity (DMS production) in summertime [*Gondwe et al.*, 2004]. Second, no high resolution AMS data analysis was performed in that study to assess the contribution of organic sulfur-containing ions. Third, meteorological conditions prevented the transport of clean oceanic air masses during the campaign. Finally, the impact of primary anthropogenic emissions was somewhat higher. Taken together, these factors prevented the resolution of an MOA-like factor although some marine influence cannot be ruled out.

[56] **Acknowledgments.** This research in the context of the MEGAPOLI project is financially supported by the European Community's Framework Program FP/2007-2011 under grant agreement 212520, as well as the Swiss National Science Foundation. SIRTA and LHVP are particularly thanked for their strong support in the field. P.F.D. is grateful for postdoctoral fellowship support from an NSF International Postdoctoral Fellowship (0701013).

References

Aiken, A. C., et al. (2007), Elemental analysis of organic species with electron ionization high-resolution mass spectrometry, *Anal. Chem.*, *79*(21), 8350–8358.

Aiken, A. C., et al. (2008), O/C and OM/OC ratios of primary, secondary, and ambient organic aerosols with high-resolution time-of-flight aerosol mass spectrometry, *Environ. Sci. Technol.*, *42*(12), 4478–4485.

Aiken, A. C., et al. (2009), Mexico City aerosol analysis during MILAGRO using high resolution aerosol mass spectrometry at the urban supersite (T0)—Part 1: Fine particle composition and organic source apportionment, *Atmos. Chem. Phys.*, *9*(17), 6633–6653.

Alfarra, M. R., et al. (2007), Identification of the mass spectral signature of organic aerosols from wood burning emissions, *Environ. Sci. Technol.*, *41*(16), 5770–5777.

Allan, J. D., et al. (2003), Quantitative sampling using an Aerodyne aerosol mass spectrometer 1. Techniques of data interpretation and error analysis, *J. Geophys. Res.*, (D3), 4090, doi:10.1029/2002JD002358.

Allan, J. D., et al. (2004), A generalised method for the extraction of chemically resolved mass spectra from aerodyne aerosol mass spectrometer data, *J. Aerosol Sci.*, *35*(7), 909–922.

Allan, J. D., et al. (2010), Contributions from transport, solid fuel burning and cooking to primary organic aerosols in two UK cities, *Atmos. Chem. Phys.*, *10*(2), 647–668.

Bates, T. S., et al. (2001), Regional physical and chemical properties of the marine boundary layer aerosol across the Atlantic during Aerosols99: An overview, *J. Geophys. Res.*, *106*(D18), 20767–20782.

Birch, M. E., and Cary, R. A. (1996), Elemental carbon-based method for occupational monitoring of particulate diesel exhaust: Methodology and exposure issues, Analyst, *121*, 1183-1190.

Canagaratna, M. R., et al. (2007), Chemical and microphysical characterization of ambient aerosols with the Aerodyne aerosol mass spectrometer, *Mass Spectrom. Rev.*, *26*(2), 185–222.

Cavalli, F., et al. (2004), Advances in characterization of size-resolved organic matter in marine aerosol over the North Atlantic, *J. Geophys. Res.*, (D24), doi:10.1029/2004JD005137.

Cavalli, F., et al. (2010), Toward a standardised thermal-optical protocol for measuring atmospheric organic and elemental carbon: The EUSAAR protocol, *Atmos. Meas. Techn.*, *3*(1), 79–89.

Ceburnis, D., et al. (2011), Quantification of the carbonaceous matter origin in submicron marine aerosol by C-13 and C-14 isotope analysis, *Atmos. Chem. Phys.*, *11*(16), 8593–8606.

Chang, R. Y. W., et al. (2011), Aerosol composition and sources in the central Arctic Ocean during ASCOS, *Atmos. Chem. Phys.*, *11*(20), 10619–10636.

Chang, R. Y. W., et al. (2012), Aerosol composition and sources in the central Arctic Ocean during ASCOS, *Atmos. Chem. Phys.*, *11*(20), 10619–10636.

Charlson, R. J., et al. (1987), Oceanic phytoplankton, atmospheric sulfur, cloud albedo and climate, *Nature*, *326*(6114), 655–661.

Chirico, R., et al. (2010), Impact of after treatment devices on primary emissions and secondary organic aerosol formation potential from in-use diesel vehicles: Results from smog chamber experiments, *Atmos. Chem. Phys.*, *10*(23), 11545–11563.

Claeys, M., et al. (2010), Chemical characterisation of marine aerosol at Amsterdam Island during the austral summer of 2006–2007, *J. Aerosol Sci.*, *41*(1), 13–22.

Crippa, M., et al. (2013), Wintertime aerosol chemical composition and source apportionment of the organic fraction in the metropolitan area of Paris, ACP, 13, 961–981.

Dall'Osto, M., et al. (2010), Aerosol properties associated with air masses arriving into the North East Atlantic during the 2008 Mace Head EUCAARI intensive observing period: An overview, *Atmos. Chem. Phys.*, *10*(17), 8413–8435.

DeCarlo, P. F., et al. (2006), Field-deployable, high-resolution, time-of-flight aerosol mass spectrometer, *Anal. Chem.*, *78*(24), 8281–8289.

DeCarlo, P. F., et al. (2010), Investigation of the sources and processing of organic aerosol over the Central Mexican Plateau from aircraft measurements during MILAGRO, *Atmos. Chem. Phys.*, *10*(12), 5257–5280.

Decesari, S., et al. (2011), Primary and secondary marine organic aerosols over the North Atlantic Ocean during the MAP experiment, *J. Geophys. Res.*, doi:10.1029/2011JD016204.

Facchini, M. C., et al. (2008a), Important source of marine secondary organic aerosol from biogenic amines, *Environ. Sci. Technol.*, *42*(24), 9116–9121.

Facchini, M. C., et al. (2008b), Primary submicron marine aerosol dominated by insoluble organic colloids and aggregates, *Geophys. Res. Lett.*, *35*(17), doi:10.1029/2008GL034210.

Fitzgerald, J. W. (1991), Marine aerosols: A review, *Atmos. Environ. Part A. General Topics*, *25*(3/4), 533–545.

Freutel, F., et al. (2013), Aerosol particle measurements at three stationary sites in the megacity of Paris during summer 2009: Meteorology and air mass origin dominate aerosol particle composition and size distribution, ACP, 13, 933–959.

Ge, X., et al. (2012a), Primary and secondary organic aerosols in Fresno, California during wintertime: Results from high resolution aerosol mass spectrometry, *J. Geophys. Res.*, doi:10.1029/2012JD018026.

Gondwe, M., et al. (2004), Comparison of modeled versus measured MSA : nss SO4 = ratios: A global analysis, *Global Biogeochem. Cycles*, *18*(2), doi:10.1029/2003GB002144.

Gros, V., et al. (2011), Volatile organic compounds sources in Paris in spring 2007. Part I: Qualitative analysis, *Environ. Chem.*, *8*(1), 74–90.

Haeffelin, M., et al. (2005), SIRTA, a ground-based atmospheric observatory for cloud and aerosol research, *Ann. Geophys.*, *23*(2), 253–275.

Harrison, R. M., et al. (2012), Atmospheric chemistry and physics in the atmosphere of a developed megacity (London): An overview of the REPARTEE experiment and its conclusions, *Atmos. Chem. Phys.*, *12*(6), 3065–3114.

He, L. Y., et al. (2010), Characterization of high-resolution aerosol mass spectra of primary organic aerosol emissions from Chinese cooking and biomass burning, *Atmos. Chem. Phys.*, *10*(23), 11535–11543.

Heringa, M. F., et al. (2012), A new method to discriminate secondary organic aerosols from different sources using high-resolution aerosol mass spectra, *Atmos. Chem. Phys.*, *12*, 2189–2203.

Hildebrandt, L., et al. (2010), Aged organic aerosol in the Eastern Mediterranean: The Finokalia Aerosol Measurement Experiment-2008, *Atmos. Chem. Phys.*, *10*(9), 4167–4186.

IPCC (2007), Fourth assessment report: The physical science basis, working group I, Final report, Geneva, Switzerland, available at: http://www.ipcc.ch/ipccreports/ar4-wg1.htm, 2007.

Jaffrezo, J. L., et al. (1998), Carboxylic acids measurements with ionic chromatography, *Atmos. Environ.*, *32*(14-15), 2705–2708.

Kroll, J. H., and J. H. Seinfeld (2008), Chemistry of secondary organic aerosol: Formation and evolution of low-volatility organics in the atmosphere, *Atmos. Environ.*, *42*(16), 3593–3624.

Laborde, M., et al. (2012), Black carbon physical properties and mixing state in the European megacity Paris, *ACPD*, *12*, 25121–25180.

Laden, F., et al. (2000), Association of fine particulate matter from different sources with daily mortality in six US cities, *Environ. Health Perspect.*, *108*(10), 941–947.

Lanz, V. A., et al. (2007), Source apportionment of submicron organic aerosols at an urban site by factor analytical modelling of aerosol mass spectra, *Atmos. Chem. Phys.*, *7*(6), 1503–1522.

Lanz, V. A., et al. (2010), Characterization of aerosol chemical composition with aerosol mass spectrometry in Central Europe: An overview, *Atmos. Chem. Phys.*, *10*(21), 10453–10471.

Liss, P. S., et al. (1997), Marine sulphur emissions, *Phil. Trans. R. Soc. Lond. B*, *352*(1350), 159–168.

Mochida, M., et al. (2002), Fatty acids in the marine atmosphere: Factors governing their concentrations and evaluation of organic films on sea-salt particles, *J. Geophys. Res., [Atmos]*, *107*(D17), doi:10.1029/2001JD001278.

Mohr, C., et al. (2011), Spatial variation of chemical composition and sources of submicron aerosol in Zurich during wintertime using mobile aerosol mass spectrometer data, *Atmos. Chem. Phys.*, *11*(15), 7465–7482.

Mohr, C., et al. (2012), Identification and quantification of organic aerosol from cooking and other sources in Barcelona using aerosol mass spectrometer data, *Atmos. Chem. Phys.*, *12*, 1649–1665.

Novakov, T., et al. (1997), Organic aerosols in the Caribbean trade winds: A natural source?, *J. Geophys. Res.*, *102*(D17), 21307–21313, doi:10.1029/97JD01487.

O'Dowd, C. D., et al. (2004), Biogenically driven organic contribution to marine aerosol, *Nature*, *431*(7009), 676–680.

Ovadnevaite, J., et al. (2012), On the effect of wind speed on submicron sea salt mass concentrations and source fluxes, *J. Geophys. Res., [Atmos]*, *117*, doi:10.1029/2010GL046083.

Paatero, P., and U. Tapper (1994), Positive matrix factorization—A nonnegative factor model with optimal utilization of error-estimates of data values, *Environmetrics*, *5*(2), 111–126.

Paatero, P., and P. K. Hopke (2003), Discarding or downweighting high-noise variables in factor analytic models, *Anal. Chim. Acta*, *490*(1-2), 277–289.

Paatero, P. (2007), User's guide for positive matrix factorization programs PMF2.EXE and PMF3.EXE University of Helsinki, Finland.

Phinney, L., et al. (2006), Characterization of the aerosol over the sub-arctic north east Pacific Ocean, *Deep-Sea Research Part II-Topical Studies in Oceanography*, *53*(20-22), 2410–2433.

Pszenny, A. A. P. (1992), Particle-size distributions of methanesulfonate in the tropical Pacific marine boundary-layer, *J. Atmos. Chem.*, *14*(1-4), 273–284.

Putaud, J. P., et al. (2000), Chemical mass closure and assessment of the origin of the submicron aerosol in the marine boundary layer and the free troposphere at Tenerife during ACE-2, *Tellus B Chem. Phys. Meteorol.*, *52*(2), 141–168.

Quinn, P. K., et al. (2000), Surface submicron aerosol chemical composition: What fraction is not sulfate?, *J. Geophys. Res, [Atmos]*, *105*(D5), 6785–6805, doi:10.1029/2006JD007582.

Rinaldi, M., et al. (2010), Primary and secondary organic marine aerosol and oceanic biological activity: Recent results and new perspectives for future studies, *Advances in Meteorology*, doi:10.1155/2010/310682.

Russell, L. M., et al. (2010), Carbohydrate-like composition of submicron atmospheric particles and their production from ocean bubble bursting, *Proc. Natl. Acad. Sci. U. S. A.*, *107*(15), 6652–6657.

Sciare, J., et al. (2003), Aerosol sources and their contribution to the chemical composition of aerosols in the Eastern Mediterranean Sea during summertime, *Atmos. Chem. Phys.*, *3*, 291–302.

Sciare, J., et al. (2009), Long-term observations of carbonaceous aerosols in the Austral Ocean atmosphere: Evidence of a biogenic marine organic source, *J. Geophys. Res.*, *114*, doi:10.1029/2009JD011998.

Sciare, J., et al. (2010), Comparison between simulated and observed chemical composition of fine aerosols in Paris (France) during springtime: Contribution of regional versus continental emissions, *Atmos. Chem. Phys.*, *10*(24), 11987–12004.

Sciare, J., et al. (2011), Large contribution of water insoluble secondary organic aerosols in the region of Paris (France) during wintertime, *J. Geophys. Res., [Atmos]*, *116*, doi:10.1029/2011JD015756.

Seinfeld, J. H., and S. N. Pandis (2006), Atmospheric Chemistry and Physics: From Air Pollution to Climate Change, 2nd ed., 31–32, John Wiley & Sons, Inc., New York.

Setyan, A., et al. (2012), Characterization of submicron particles influenced by mixed biogenic and anthropogenic emissions using high-resolution aerosol mass spectrometry: Results from CARES, *Atmos. Chem. Phys.*, *12*, 8131–8156.

Sun, Y. L., et al. (2011), Characterization of the sources and processes of organic and inorganic aerosols in New York City with a high-resolution time-of-flight aerosol mass spectrometer, *Atmos. Chem. Phys.*, *11*(4), 1581–1602.

Ulbrich, I. M., et al. (2009), Interpretation of organic components from positive matrix factorization of aerosol mass spectrometric data, *Atmos. Chem. Phys.*, *9*(9), 2891–2918.

Viana, M., et al. (2009), Chemical tracers of particulate emissions from commercial shipping, *Environ. Sci. Technol.*, *43*(19), 7472–7477.

Virkkula, A., et al. (2006), Chemical size distributions of boundary layer aerosol over the Atlantic Ocean and at an Antarctic site, *J. Geophys. Res.*, (D5), doi:10.1029/2004JD004958.

Zhang, Q., et al. (2005), Deconvolution and quantification of hydrocarbon-like and oxygenated organic aerosols based on aerosol mass spectrometry, *Environ. Sci. Technol.*, *39*(13), 4938–4952.

Zhang, Q., et al. (2007), Ubiquity and dominance of oxygenated species in organic aerosols in anthropogenically-influenced Northern Hemisphere midlatitudes, *Geophys. Res. Lett.*, *34*(13).

Zhang, Q., et al. (2011), Understanding atmospheric organic aerosols via factor analysis of aerosol mass spectrometry: A review, *Anal. Bioanal. Chem.*, *401*(10), 3045–3067, doi:10.1029/2007GL029979.

Zorn, S. R., et al. (2008), Characterization of the South Atlantic marine boundary layer aerosol using an Aerodyne aerosol mass spectrometer, *Atmos. Chem. Phys.*, *8*(16), 4711–4728.